FEM simulation and reverse engineering of an Electronic Railway Wheel Detector

J. J. Munoz[1], S. Karoui[1]

1. SNCF Réseau, DGII Telecommunications Department, La Plaine Saint Denis, France

Abstract: The electronic wheel detector is a device that has been widely used at SNCF (Société Nationale de Chemins de fer Français) for train passage detection, which constitutes a primary task in coordination of railway signaling system. The detectors have been deployed in the company for at least three decades; however, some dysfunctions have been noticed in their functioning, apparently due to their sensibility to external magnetic fields. This is why the EMC team at SNCF's Telecommunications Department has been working on developing a model of these detectors, so simulation scenarios reproducing their functioning could be implemented to determine potential sources of malfunctioning. This paper presents an initial finite element method modeling approach of these detectors using COMSOL Multiphysics®.

Keywords: *Electromagnetic simulation, Electromagnetic compatibility, FEM simulation*

1. Introduction

Electronic wheel detectors constitute an essential part of electronic pedals, which are devices that allow detecting trains' passage. They are connected to signaling circuits and they play an essential role in railway system security [1, 2]. In recent years, some dysfunctions have been noticed in their functioning, apparently due to their sensibility to external magnetic fields. Nevertheless, knowledge concerning the sources of such malfunctioning remains limited, which justifies the realization of different studies that could lead to a better understanding of this problematic.

These detectors have been deployed in SNCF for already 3 decades. Due to their oldness, they're no longer fabricated and most available technical documents don't contain the necessary information for their numerical modeling. This is why a reverse engineering approach was adopted. In such approach, a physical exemplary of the detector was taken and its dimensions were used for developing a geometrical numerical model. By using this geometrical information and by combining it with our knowledge of the functioning of detectors, it was possible to develop a model allowing the reproduction of the device's behavior.

Electronic detectors mainly consist in a "U" ferrite where two coils are placed (each coil is placed at a different side of the "U"). Such coils are connected in series in a way the magnetic flux they produce is additive, and they're connected as well to a capacitor that allows forming an oscillating LC series circuit. The resonance frequency of such circuit is typically 39 kHz or 50 kHz and it depends on the detector's reference.

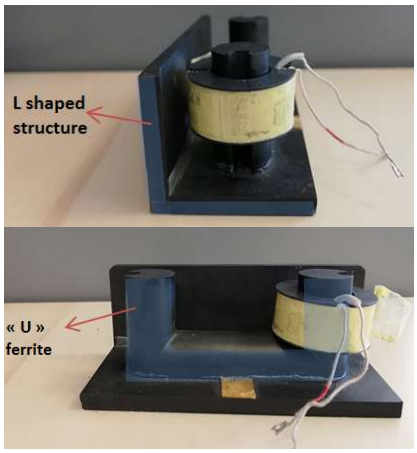

Figure 1. Physical exemplary of the electronic detector (D39). Only one of the coils is present and the capacitor has been removed.

When a train passes, wheels close the "U". An augmentation in the magnetic flux through the detector is expected and the circuit's equivalent inductance consequently increases. Therefore, there is an augmentation of the circuit's impedance that results in a voltage drop at the terminals of the detector; this drop is then analyzed by a signal processing block which will translate the described phenomena into a train's passage [2].

Previous related work at SNCF included a 2D modeling of the device using Comsol Multiphysics® [3]. Even though such approach allows fairly

reproducing the functioning of the detector, its precision as well as its usage in further studies are very limited.

This paper shows a tridimensional FEM modeling approach of the detector by using COMSOL Multiphysics software®.

2. Modeling methodology

2.1. Geometry and material

There aren't any available data or measurements concerning the ferrite composing the detector. In absence of such information, we proposed to model the ferrite by using the "Soft Iron" material from Comsol Multiphysics materials library. As it can be seen in figure 2, using such material introduces a non-linear relation between fields $\vec{H}$ and $\vec{B}$. Using this curve implies performing an approximation of a non-linear function in every solver's iteration, which might lead to a high computational effort. As long as the material doesn't saturate, a simpler linear relation $\vec{B} = \mu_r \mu_0 H$ can be used. This helps reducing the required simulation time; nevertheless, precision of calculated results is lowered when the operating point of the detector isn't at the linear zone of the B-H curve.

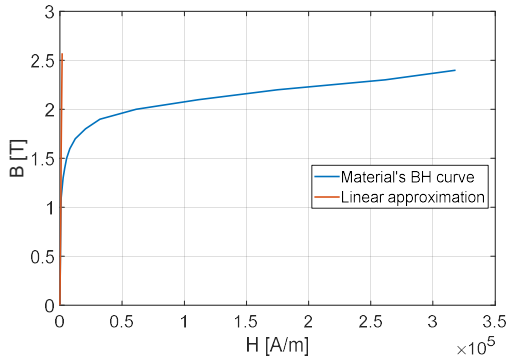

Figure 2. B-H curve of soft iron

3D geometry was built directly on COMSOL Multiphysics and it was inspired on the physical exemplary from figure 1. Such exemplary corresponds to a D39 detector (a detector which resonance frequency is around 39 kHz).

Initially, a model considering exclusively the "U" ferrite was built. It can be seen, however, that the "U" ferrite is mounted on an L-shaped structure which inclusion might have an influence on the overall simulation results (see Figure 1). Indeed, since the "L" structure is made from the same material as the "U", distribution of simulated magnetic flux in the ferrite is affected by the consideration of this L-shaped base and thus, results may significantly vary with respect to the initial case. Inclusion of this structure leads to a more realistic representation of the device; it also constitutes an additional reason for using a 3D modeling approach, since its inclusion wouldn't have been possible in a 2D model.

2.2. Simulation setup

Our electromagnetic problem is set at low frequencies (the resonance frequency of the detector is 39 kHz). Therefore, the COMSOL module that best adapts to our modeling is the AC/DC module. In such module, the magnetic fields interface allows calculating the magnetic field generated by the device as well as defining the way coils are modeled. This interface can also be used to analyze the detector's response when immersed in an external magnetic field.

Geometric coils can be coupled to a circuit model by using the electrical circuits interface. In addition, the detector's capacitor can easily be included in the model as a lumped element.

More details about the model's implementation by using the previous interfaces are given below:

2.2.1. Magnetic fields interface

- Ampère's law is used for computing magnetic fields in all calculation domain. Since the electronic wheel detector corresponds to a low-frequency problem, variations in electric flux density can be neglected and Ampère's law becomes:

$$\nabla \times \vec{H} = \vec{J}$$

  This equation is solved for magnetic vector potential $\vec{A}$, a vector field such that $\vec{B} = \nabla \times \vec{A}$. The relation between $\vec{B}$ and $\vec{H}$ depends on the material properties of the region the equations are solved in. For the detector's ferrite, such relation is given by the curve in figure 2.

- Multiple possibilities for modeling coils are available in Comsol's magnetic fields interface. In our case, precisely drawing and meshing the coils' geometry would have introduced a significant computational effort. For this reason, it was preferred to consider numeric and homogeneous coils. This allows representing

them as an equivalent current density; only the number of turns and the current direction must be specified in the modeling interface. Direction of current in each coil is chosen so that magnetic flux of both coils is additive (this can be verified by simply applying the right-hand rule).

- Since there are multiple $\vec{A}$ fields satisfying $\vec{B} = \nabla \times \vec{A}$, the condition $\nabla \cdot \vec{A} = 0$ is imposed in all regions of calculation domain to guarantee the unicity of the solution.

- Calculation domain is a rectangular box containing the geometry of the device. Magnetic insulation boundary conditions were applied on such box boundaries to force magnetic fields to be zero when far from the detector.

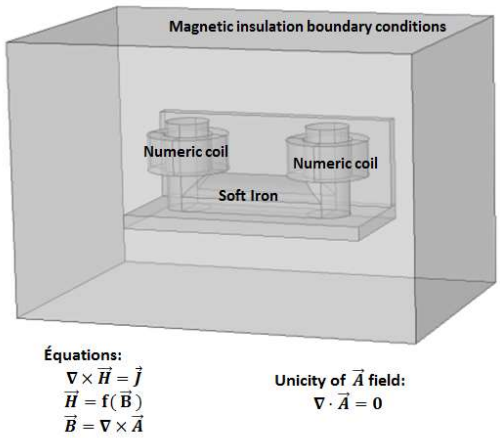

Figure 3. Numerical simulation setup.

2.2.2. Electrical circuits interface

In this interface, the geometric model is translated into an electrical circuit. The previously defined coils can be integrated to the circuit through the "External I vs. U" option. An external resistance to represent losses in conductors and the detector's capacitor are added as lumped elements in order to complete the circuital model.

One recalls that the resonance angular frequency ω_r, of an LC circuit satisfies the relation $\omega_r L - \frac{1}{\omega_r C} = 0$.

2.3. Mesh

A tetrahedral mesh was used in all our simulations. Mesh size was set by launching a parametric simulation on the mesh. Results of such simulation will be discussed in next session.

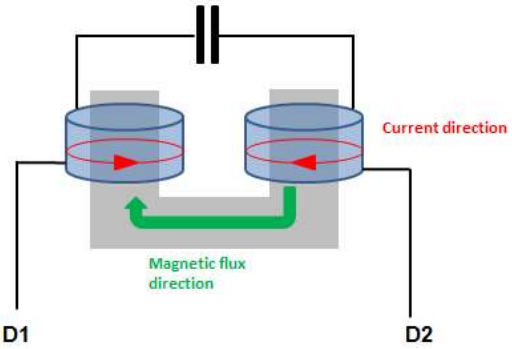

Figure 4. Circuital representation of the detector.

3. Simulation results

A simulation case was defined to verify that the model corresponds to the theoretical characteristics of the detector. Since the device is equivalent to an RLC circuit which LC part resonates at 39 KHz, if an echelon excitation is applied between terminals D1 and D2 (see figure 4) so that the system operates in its linear region and if the conductor's resistance is not neglected, the system transient response should correspond to that of a second-order underdamped system. This means the circuit's voltages and currents should be sinusoids which amplitudes decrease in time and which frequency equals the resonance frequency of the detector. In consequence, this frequency should be close to 39 kHz for our model to correspond to the theoretical functioning of the device.

The following scenarios were tested:

- **Variation in model's geometrical details**: A first scenario considers a "reduced" geometrical model of the detector where the L-shaped structure on which the "U" is mounted isn't considered. A second scenario aims to determine whether the inclusion of the "L" changes the simulation results in a significant way or not.

  Results allow validating theoretical characteristics of the device. Indeed, the detector's current transient response corresponds to the description given above and in both cases the resonance frequency is close to 39 kHz. It can be stated, however, that this frequency changes in

function of the simulation scenario, and that it is much closer to 39 kHz in the second scenario, where the L-shaped structure is simulated (the calculated frequency was 41666 Hz and 38910 Hz in the first and the second scenario, respectively).

When considering the "L" structure, new paths for magnetic flux are created and the way $\vec{B}$ field distributes in the structure changes. This results in an augmentation on the circuit's inductance that lowers its resonance frequency with respect to the case in which the "L" is neglected.

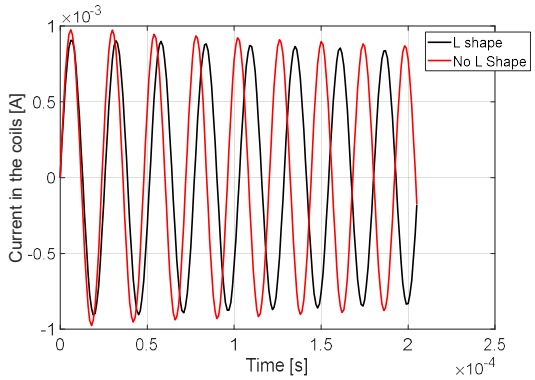

Figure 5. Current in the coils

Figure 5 shows the current circulating through the coils and Figures 6 and 7 show the norm and direction of $\vec{B}$ field for both simulation scenarios at the point where this norm reaches its maximum.

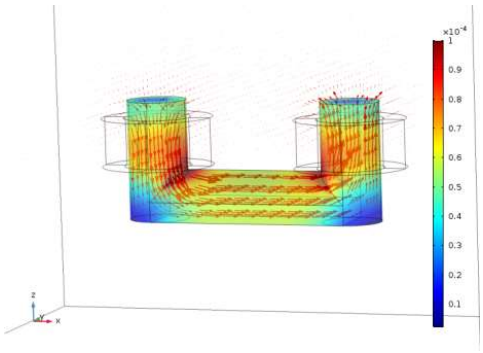

Figure 6. $\vec{B}$ field in the first simulation scenario.

- **Passage of a wheel:** A third scenario consisted in placing a ferromagnetic structure on top of the device. Such structure represents the part of the wheel that interferes with the detector. It was initially modeled as a rectangular block and, since no data concerning its material properties were available, it was defined as being constituted of soft iron.

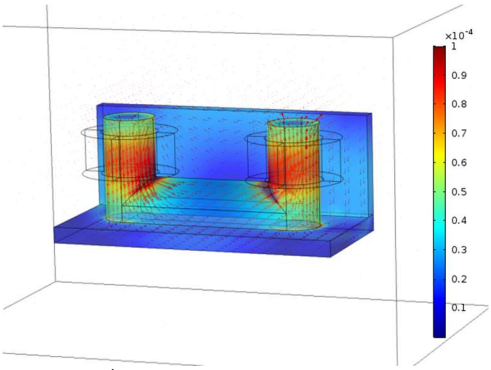

Figure 7. $\vec{B}$ field in the second simulation scenario.

The passage of a wheel closes the magnetic circuit and increases the detector's inductance, which decreases its resonance frequency. In consequence, when applying an echelon voltage, a slower transient and a smaller current are expected with respect to the case in which the magnetic circuit is open. In addition, the inductance augmentation becomes less important when the gap between the detector and the structure is increased. This allows defining the sensibility zone of the detector, which corresponds to the interval of distances measured from the top of the detector for which a passing wheel would generate a detectable changement in the circuit's impedance at 39 kHz.

Figure 8 shows the imaginary part of the detector's impedance as a function of frequency for different gap values. It can be verified that the greater the gap, the closer the resonance frequency is to 39 kHz, which corresponds to the case in which the magnetic circuit is open. It is estimated that the detector is perturbed by wheels passing at a maximal distance of approximately 4cm from its top, which is coherent with the information provided in different technical documents [4].

Even though simulation results are coherent with the detector's functioning principle, in order to more accurately determining its sensibility zone with respect to a passing wheel it is necessary to have a better representation of the interfering structure in terms of its geometry and material constitution.

- **Application of an external field**: A fourth scenario consisted in setting to zero the voltage between the detector's terminals and applying at the same time an echelon external magnetic field. This simulation aims to analyze the impact external fields may have on the detector.

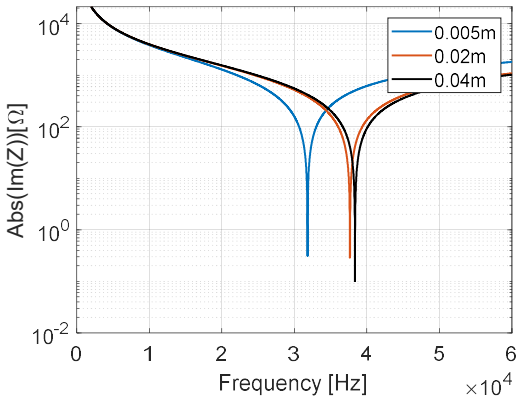

Figure 8. Impedance of the detector for different gap values (only the imaginary part is considered).

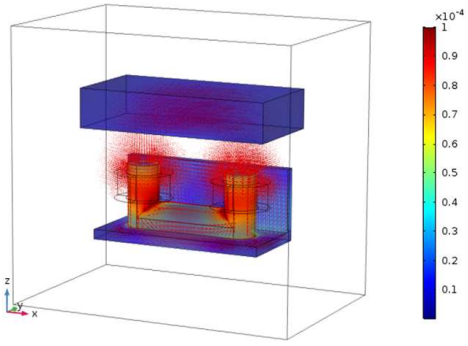

Figure 9. Calculated magnetic field in third simulation scenario.

It could be stated that even though no tension is applied between the terminals, the external magnetic field induces a transient current in the coils. Such current is similar to the one described in the second simulation scenario (see figure 10); however, the amplitude of oscillations may change in function of the external field magnitude and direction.

3.1. Mesh convergence

A parametric analysis on mesh size was performed to test mesh convergence. Figure 10 shows the calculated current for two different types of mesh in the second simulation scenario listed above. A coarse mesh with maximal and minimal element size of 0.05m and 0.005m, respectively, and a finer mesh with maximal and minimal element size of 0.01m and 0.001m were used in such simulation.

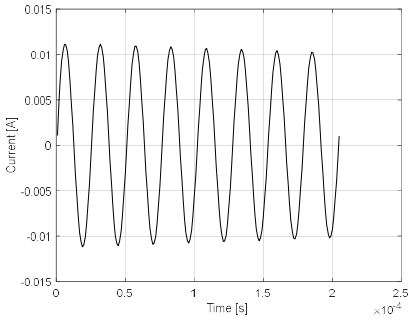

Figure 10. Induced transient current by an external 0.1T magnetic induction applied on x-axis direction.

Results show convergence of calculated quantities in terms of mesh size. Also, simulation using the coarse mesh takes about nine times less to run, which represents a considerable gain in simulation time without great loss in terms of results precision.

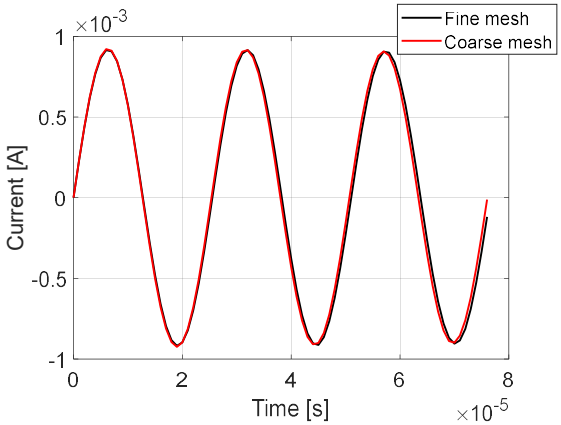

Figure 10. Calculated current for different mesh sizes in the second simulation scenario.

4. Conclusion and further work

Simulation results are coherent with the detector's theoretical functioning principle. It was verified through simulation that this device corresponds to an RLC circuit which resonance frequency is about 39 kHz. It was also seen that simulation results were sensible to geometry variations in the detector; indeed, the inclusion of the L-shaped base allowed obtaining a resonance frequency which is closer to its theoretical

value than the simulation case in which such structure was ignored (the error percentage with respect to 39KHz was 0.23% and 6.83%, respectively).

Simulation scenarios were developed to approximate what it would be a wheel's passage. It was verified how closing the magnetic circuit increased the circuit's impedance and it was seen how the gap between the wheel and the detector could vary such augmentation. Such gap must guarantee the detector will be interfered when the train passes; otherwise it would be unable to detect it. However, to appropriately determine the influence zone of detectors it is necessary to have a better description of wheels geometry and electromagnetic material properties. It was also verified that external fields may influence the overall behavior of detectors, and therefore placing them in complex electromagnetic environments could be a potential source of malfunctioning. Exact sources of dysfunctions can't however be determined with the simulations we dispose of so far.

Further work includes cooperating with signaling and measurements departments of SNCF. Information about surrounding electromagnetic environment of the places where failures in detector's functioning were noticed is necessary to create modeling conditions allowing the determination of potential malfunctioning sources. Also, for our model to be used in such simulations, it would be convenient to validate our results with available measurements. It would also be interesting to analyze modeling possibilities to turn our geometry into dynamic in order to better study a wheel's passage.

References

1. Guillaume Éric, Électronique modernisée des pédales D50, 2015
2. Fournier Patrice, Détecteur électronique de roue type D39-D50 (internal SNCF document), 2017
3. Ndiaye Abdou Coura, Modélisation du comportement électromagnétique des détecteurs électroniques de roues D39-D50, École Polytechnique, 2018.
4. EPSF, Protocole de vérification de la compatibilité des matériels roulants avec les détecteurs électroniques, 2016.
5. Peetenut Triwong. Modélisation numérique 3D des phénomènes couplés dans les procédés d'élaboration par induction : couplage faible et couplage fort. Institut National Polytechnique de Grenoble – INPG, 2008.
6. Frei Walter, Solutions to linear systems of equations: direct and iterative solvers, 2013.